

## Stripes Induced by Orbital Ordering in Layered Manganites

Takashi Hotta,<sup>1</sup> Adrian Feiguin,<sup>2</sup> and Elbio Dagotto<sup>2</sup>

<sup>1</sup>*Institute for Solid State Physics, University of Tokyo, 5-1-5 Kashiwa-no-ha, Kashiwa, Chiba 277-8581, Japan*

<sup>2</sup>*National High Magnetic Field Laboratory, Florida State University, Tallahassee, Florida 32306*

(Received 6 December 2000)

Spin-charge-orbital ordered structures in doped layered manganites are investigated using an orbital-degenerate double-exchange model tightly coupled to Jahn-Teller distortions. In the ferromagnetic phase, unexpected diagonal stripes at  $x = 1/m$  ( $m = \text{integer}$ ) are observed, as in recent experiments. These stripes are induced by the orbital degree of freedom, which forms a staggered pattern in the background. A  $\pi$  shift in the orbital order across stripes is identified, analogous to the  $\pi$  shift in spin order across stripes in cuprates. At  $x = 1/4$  and  $1/3$ , another nonmagnetic phase with diagonal static charge stripes is stabilized at intermediate values of the  $t_{2g}$ -spins exchange coupling.

DOI: 10.1103/PhysRevLett.86.4922

PACS numbers: 75.30.Kz, 71.15.-m, 75.10.-b, 75.50.Ee

Manganese oxides are currently attracting considerable attention [1], due to the complex interplay among spin, charge, and orbital degrees of freedom, which induces a rich phase diagram as well as colossal magnetoresistant (CMR) properties. There are clearly two types of dominant states in these compounds. For example, in perovskite manganites such as  $\text{La}_{1-x}\text{Ca}_x\text{MnO}_3$ , in the region  $0.22 < x < 0.5$  a ferromagnetic (FM) metallic phase is the ground state at low temperature. On the other hand, at  $x > 0.5$ , a charge-orbital-spin ordered state is stabilized. The competition between these two states is at the heart of recent theories that explain the CMR effect in manganites as arising from mixed-phase tendencies [2].

This two-phase metal-insulator competition and concomitant large MR effect occurs also at the Curie temperature  $T_C$ , at densities where a FM phase exists at low temperature. Several experiments have clearly revealed the mixed-phase characteristics of manganites near  $T_C$  [3]. While it is natural to assume that one of the competing phases is FM metallic, the properties of the insulating phase are still unknown. Recently, considerable progress has been made in this context. Just above  $T_C$  evidence for the existence of short-range *stripelike* charge ordering has been obtained with neutron diffraction and x-ray scattering studies. For  $\text{La}_{1-x}\text{Ca}_x\text{MnO}_3$  [4], “diagonal” stripes, i.e., charge ordering (CO) along the  $(1, 1, 0)$  direction [5], appear for  $0.2 \lesssim x \lesssim 0.3$ , while for  $x < 0.2$ , “bond” stripes, i.e., CO along the  $(1, 0, 0)$  or  $(0, 1, 0)$  direction, have been revealed. For  $\text{La}_{2-2x}\text{Sr}_{1+2x}\text{Mn}_2\text{O}_7$  [6], short-range bond stripes have been detected in the wide range  $0.3 \leq x \leq 0.5$ . These results lead to the intriguing possibility that the insulating phase that contributes to the CMR near  $T_C$  may also be FM but with striped features, a remarkable novel result. Such a state would be

puzzling since stripes in cuprates are associated with the creation of rivers of holes to avoid having the individual charges “fighting” against the antiferromagnetic (AFM) background. Thus in a FM state, where hole movement appears optimal, charge is naively not expected to form stripes, in contradiction with experiments.

In order to understand this puzzling complex problem, in this Letter the two-dimensional (2D) double-exchange (DE) model coupled to Jahn-Teller (JT) phonons is investigated using unbiased computational techniques. This model has been already successful in reproducing the A-type AFM state at  $x = 0$  [7], the CE state at  $x = 0.5$  [8], and the complex structure of the  $x > 0.5$  regime [9], as observed in experiments. However, a state as exotic as containing stripes in a ferromagnetic background has not been reported until now. The present effort focuses on the properties of 2D systems, since (i) studies in three-dimensional (3D) cases are technically far more complex, and (ii) stripe structures identified experimentally in bilayer and 3D manganites are here observed in 2D systems as well. Our main result is the stabilization of *FM states with stripe order* at  $x = 1/m$  ( $m = \text{integer}$ ), a surprising result whose origin lies in the concomitant orbital order.

Regarding single-layered manganites  $\text{La}_{1-x}\text{Sr}_{1+x}\text{MnO}_4$ , the undoped compound is AFM [10], while at  $x \sim 0.5$  a CE-type AFM CO phase has been identified [11]. However, for  $0.0 < x < 0.5$ , a complex “spin glass” behavior has been experimentally observed [12], indicating that the 2D ground-state properties are basically unknown. Our results below also indicate that stripe states with CE-like AFM characteristics may exist at  $x = 1/4$  and  $1/3$ , and they could be important for the physics of single-layered compounds in non-FM regimes.

The Hamiltonian studied here is

$$\begin{aligned}
 H = & - \sum_{i\mathbf{a}\gamma\gamma'\sigma} t_{\gamma\gamma'}^{\mathbf{a}} d_{i\gamma\sigma}^\dagger d_{i+\mathbf{a}\gamma'\sigma} - J_H \sum_i \mathbf{s}_i \cdot \mathbf{S}_i + J_{AF} \sum_{\langle i,j \rangle} \mathbf{S}_i \cdot \mathbf{S}_j \\
 & + \lambda \sum_i (Q_{1i}\rho_i + Q_{2i}\tau_{xi} + Q_{3i}\tau_{zi}) + (1/2) \sum_i (\beta Q_{1i}^2 + Q_{2i}^2 + Q_{3i}^2), \quad (1)
 \end{aligned}$$

where  $d_{i\alpha\sigma}$  ( $d_{ib\sigma}$ ) is the annihilation operator for an  $e_g$  electron with spin  $\sigma$  in the  $d_{x^2-y^2}$  ( $d_{3z^2-r^2}$ ) orbital at site  $\mathbf{i}$ , and  $\mathbf{a}$  is the vector connecting nearest-neighbor (NN) sites. The first term represents the NN hopping of  $e_g$  electrons with the amplitude  $t_{\gamma\gamma'}$  between  $\gamma$  and  $\gamma'$  orbitals along the  $\mathbf{a}$  direction ( $t_{ga}^x = -\sqrt{3}t_{ab}^x = -\sqrt{3}t_{ba}^x = 3t_{bb}^x = 1$  for  $\mathbf{a} = \mathbf{x}$  and  $t_{aa}^y = \sqrt{3}t_{ab}^y = \sqrt{3}t_{ba}^y = 3t_{bb}^y = 1$  for  $\mathbf{a} = \mathbf{y}$ , in  $t_{aa}^x$  energy units). In the second term, the Hund coupling  $J_H (>0)$  links  $e_g$  electrons with spin  $\mathbf{s}_i = \sum_{\gamma\alpha\beta} d_{i\gamma\alpha}^\dagger \boldsymbol{\sigma}_{\alpha\beta} d_{i\gamma\beta}$  ( $\boldsymbol{\sigma}$  are the Pauli matrices) with the localized  $t_{2g}$  spin  $\mathbf{S}_i$ , assumed classical and normalized to  $|\mathbf{S}_i| = 1$ . The third term is the AFM coupling  $J_{AF}$  between NN  $t_{2g}$  spins [13]. The fourth term couples  $e_g$  electrons and  $\text{MnO}_6$  octahedra distortions,  $\lambda$  is the dimensionless coupling constant,  $Q_{1i}$  is the breathing-mode distortion,  $Q_{2i}$  and  $Q_{3i}$  are, respectively,  $(x^2 - y^2)$ - and  $(3z^2 - r^2)$ -type JT-mode distortions,  $\rho_i = \sum_{\gamma,\sigma} d_{i\gamma\sigma}^\dagger d_{i\gamma\sigma}$ ,  $\tau_{xi} = \sum_{\sigma} (d_{i\alpha\sigma}^\dagger d_{ib\sigma} + d_{ib\sigma}^\dagger d_{i\alpha\sigma})$ , and  $\tau_{zi} = \sum_{\sigma} (d_{i\alpha\sigma}^\dagger d_{i\alpha\sigma} - d_{ib\sigma}^\dagger d_{ib\sigma})$ . The fifth term is the potential for distortions, where  $\beta$  is the ratio of spring constants for breathing and JT modes, treated here adiabatically [14].

First let us clarify the charge and orbital structure in the FM phase, the main issue of this paper. If lattice distortions are not correlated in different sites, holes will be simply distributed as uniformly as they can to lower the ground state energy. Namely, the stabilization of charge inhomogeneous structure such as stripes in the FM phase requires a proper treatment of the *cooperative* JT effect. A simple way to include such an effect is to optimize the displacement of oxygen ions  $u_i^a$  along the  $\mathbf{a}$  axis at site  $\mathbf{i}$ , instead of local distortions [15]. Results at large  $\lambda$  for the FM phase are shown in Fig. 1. Using relaxation techniques

to optimize  $\{u\}$ 's, *diagonal stripes* can be clearly observed even in a spin FM regime, a surprising result. The key ingredient to understanding the presence of stripes in a spin magnetized phase is the presence of the concomitant *staggered* orbital order. Individual holes doped into the  $x = 0$  FM orbital-ordered (OO) state produce a distortion of the ordered background. This energy lost is minimized if holes share the distorted regions, forming complex patterns such as stripes. A similar reasoning is usually applied to the rationalization of stripe formation in nickelates and cuprates [16], with the important conceptual difference that in those compounds the background in which the stripes are created is spin AFM, i.e., the real spin is active, while in the present study the spin is FM and the orbital background is active. If the orbital degree of freedom is associated to a "pseudospin" up and down, then an analogy between manganites and nickelates/cuprates can be established, replacing the real spin of the latter by the orbital degree of freedom of the former. In fact, with this analogy the pseudospin and charge structure at  $x = 1/4$  [Fig. 1(c)] becomes the same as the real-spin and charge stripe structure of hole-doped  $\text{La}_2\text{NiO}_4$ , at the same hole density [17]. In the stripe phase, a gap of the order of the JT energy opens around the Fermi level [see Fig. 1(d)]. Thus, "pseudogap" features may be expected as precursors for stripe formation even at high temperatures such as  $T_C$ .

Note that the stable charge-orbital stripes with the arrangement of Fig. 1 can appear when the distance  $d$  between diagonal hole arrays is equal to  $ma_0$ , where  $m$  is an integer and  $a_0$  is the lattice constant along the  $a$  axis. Since  $d = a_0/x$  from Fig. 1,  $x$  should be equal to  $1/m$  for the appearance of stable diagonal charge stripes. For  $1/(m+1) < x < 1/m$ , it seems possible (but at this early stage it is a conjecture) that a mixed phase of two charge-orbital ordered states with  $x = 1/(m+1)$  and  $1/m$  appears, consistent with the phase separation scenario [2] and also with recent synchrotron x-ray scattering measurements [18]. Based on this scenario, the charge ordering observed in experiments at  $x \sim 0.3$  in the FM regime may be understood as a mixture of diagonal stripes at  $x = 1/4$  and  $1/3$  [Figs. 1(b) and 1(c)], if those patterns are assumed to be stacked along the  $z$  axis due to the influence of  $J_{AF}$ , a reasonable assumption based on previous  $x = 0.5$  calculations [8]. In the orbital correlation function  $T^z(\mathbf{q}) = \sum_{i,j} e^{i\mathbf{q}\cdot(\mathbf{i}-\mathbf{j})} \langle \tau_{zi} \tau_{zj} \rangle$ , peaks appear at  $(\pi \pm \delta_m, \pi \pm \delta_m)$  with  $\delta_m = (1 - 2/m)\pi$ . The deviation from  $(\pi, \pi)$  for  $m > 2$  is caused by a  $\pi$  shift in the orbital order across the stripe (Fig. 1), and it can be informally referred to as "orbital incommensurability" by analogy to the spin incommensurability found in cuprates and nickelates. It is important to remark that the present idealized charge stripes will likely be destabilized by thermal and/or quantum fluctuations. Thus, in actual materials, it is expected that the stripes will be *dynamical* as in cuprates and only vestiges of stripes may be detected [19], together with pseudogap features, consistent with the phase separation tendency for  $1/(m+1) < x < 1/m$ .

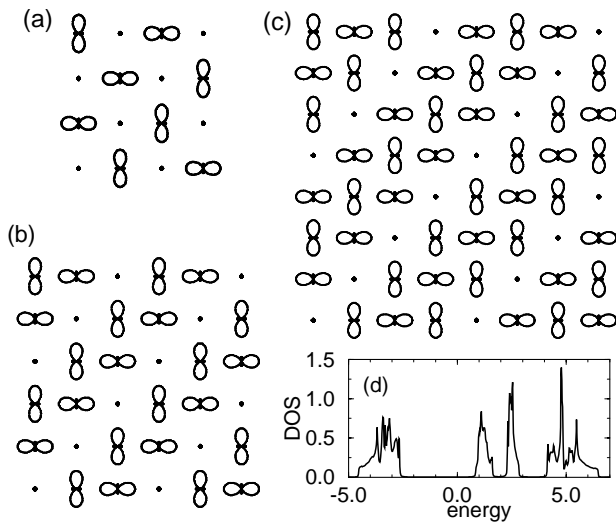


FIG. 1. Orbital arrangement in the CO FM phase at (a)  $x = 1/2$ , (b)  $1/3$ , and (c)  $1/4$  with  $\lambda = 2.0$ . The charge density in the lower-energy orbital is shown, with the size of the orbital being in proportion to this density. (d) Total density of states vs energy for  $x = 1/3$  and  $\lambda = 2.0$ .

Now let us consider the charge-orbital structure in the AFM phase by using *noncooperative* JT phonons. This will allow us to report yet another striped state which could be observed experimentally, this time with an overall zero magnetization. As found at  $x = 1/2$  [8], the AFM phase such as CE-type state is not sensitive to the JT phonons treatment, since there exists a strong constraint due to the DE mechanism for the  $e_g$  electron kinetic motion, masking differences in the character of JT phonons. Note, however, that both the local lattice distortion and  $t_{2g}$  spin direction should be determined independently at each site by optimizing the total energy. Using relaxation techniques to optimize  $\{Q\}$ 's and  $\{S\}$ 's at fixed electronic density [20], the phase diagram at  $x = 1/4$  has been here obtained [Fig. 2(a)]. Its overall features can be understood from the competition between the  $e_g$  electron kinetic energy and magnetic energy of  $t_{2g}$  spins regulated by  $J_{AF}$ . At small  $J_{AF}$  the system becomes FM to improve hole movement, and a metal-insulator transition occurs at a critical value of  $\lambda$ , separating FM CO and FM charge-disordered (CD) states. In the other limit of large  $J_{AF}$ , an AFM phase is stabilized since the magnetic energy among  $t_{2g}$  spins dominates. The most interesting result of Fig. 2(a) is that at *intermediate* values of  $J_{AF}$ , a novel spin-ordered state analogous to the CE-type phase at  $x = 1/2$  has been found. The complex optimized spin pattern is shown in Fig. 2(b). A similar CE-like spin arrangement is also found at  $x = 1/3$  [see Fig. 2(c)] [21]. These configurations are here called the “zigzag” AFM (Z-AFM) states, since  $t_{2g}$  spins form one-dimensional (1D) zigzag paths where  $e_g$  kinetic energy is gained, stacking with antiparallel spins in the direction perpendicular to those paths to gain magnetic energy. Since this Z-AFM phase can take

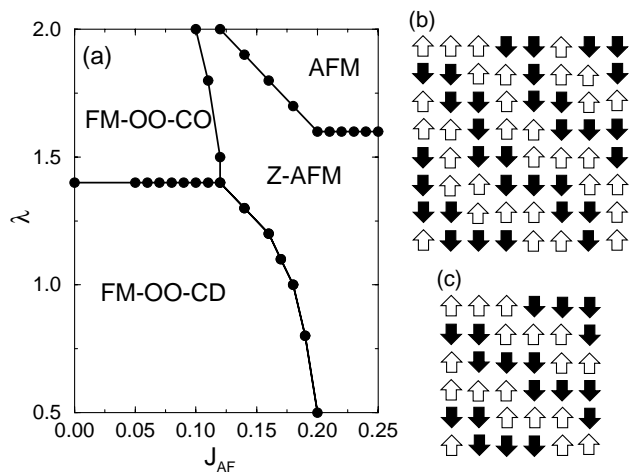


FIG. 2. (a) Zero-temperature phase diagram at  $x = 1/4$  and large  $J_H$  (see text for notation). The metallic FM-CD and insulating FM-CO boundary is obtained monitoring the average JT distortions with increasing  $\lambda$ . (b) Ground-state spin pattern on an  $8 \times 8$  cluster for intermediate values of  $J_{AF}$  at  $x = 1/4$  [Z-AFM phase in (a)]. Open and solid arrows indicate up and down spins, respectively. (c) Spin arrangement on the  $6 \times 6$  cluster in the Z-AFM regime at  $x = 1/3$ .

partial advantage of both energies, it is reasonable that it is stabilized in between the FM and AFM phases.

Consider now the charge and orbital structures of the phases in Fig. 2(a). In the FM phase, for the values of  $\lambda$  investigated, an OO phase appears (not shown), irrespective of the charge structure. As mentioned above, for noncooperative JT phonons, holes are distributed uniformly to lower the ground state energy, compatible with the concomitant orbital order. In the Z-AFM phase, the charge-orbital arrangements for large  $\lambda$  are schematically shown in Figs. 3(a) and 3(b) for  $x = 1/4$  and  $1/3$ , respectively. The local charge density is found to be constant along the diagonal directions denoted by the broken lines in Fig. 3(a). This result indicates a tendency toward the formation of diagonal charge stripes in the Z-AFM phase for  $x = 1/3$  and  $1/4$ . In Fig. 3(c), the local charge densities on the diagonal lines,  $n(\delta_1)$ ,  $n(\delta_2)$ , and  $n(\delta_3)$ , are shown vs  $\lambda$ . At small  $\lambda$ , diagonal charge stripes are observed, concomitant with a peak around  $\mathbf{q} = (\pi/2, \pi/2)$  in the charge correlation function  $n(\mathbf{q})$  [22]. On the other hand, at large  $\lambda$ ,  $n(\delta_3)$  is very small, while  $n(\delta_1)$  and  $n(\delta_2)$  are almost unity. Namely, holes are mainly located along the line  $\delta_3$ , indicating the formation of a clear diagonal charge stripe

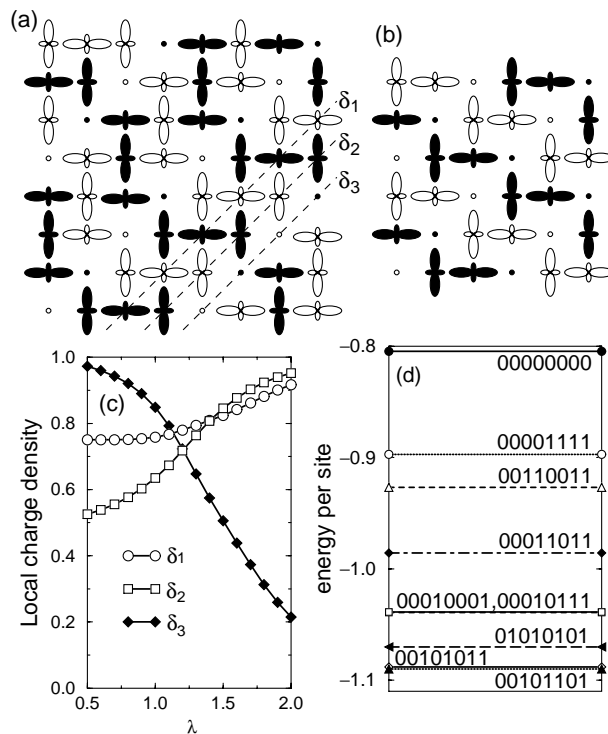


FIG. 3. (a) Schematic view of spin-charge-orbital ordering in the Z-AFM phase at large  $\lambda$  and  $x = 1/4$ . Open and solid symbols indicate up and down  $t_{2g}$  spins, respectively. The lobes indicate  $d_{3x^2-r^2}$  or  $d_{3y^2-r^2}$  orbitals in the  $\text{Mn}^{3+}$  site, and the small circles denote the hole sites in which the  $d_{x^2-y^2}$  orbital is occupied by a tiny amount of charge. (b) Same as (a), but for  $x = 1/3$ . (c) Charge densities [see (a)] vs  $\lambda$  at  $x = 1/4$  in the Z-AFM, where results at a given  $\lambda$  are  $J_{AF}$  independent. (d) Energies of several paths for  $x = 1/4$ ,  $\lambda = 0$ , and  $J_{AF} = 0.25$  in the Z-AFM regime (see text for notation).

pattern [see Fig. 3(a)], and the intensity of the  $(\pi/2, \pi/2)$  peak in  $n(\mathbf{q})$  becomes larger than at small  $\lambda$ . Note that in the Z-AFM phase the  $e_g$  electron motion is restricted to the 1D zigzag FM chains due to large  $J_H$ . When a finite electron-lattice coupling is introduced in this 1D system, a Peierls instability should occur, leading to a charge-density-wave state. Since in the Z-AFM phase the same chain is simply stacked along the diagonal direction in the  $x$ - $y$  plane, diagonal charge stripes occur naturally.

To understand the shape of the zigzag chain [Fig. 2(b)], consider the limit of  $\lambda = 0$  [8,9]. Even without phonons, by straightforward diagonalization it can be shown that the zigzag chains have a spectra corresponding to a *band insulator* due to the periodic changes in hopping amplitudes along zigzag chains ( $t_{ab}^x = -t_{ab}^y$ ), which induce gaps in the energy spectra [9]. At  $x = 1/4$ , there are nine independent possible types of zigzag chains on an  $8 \times 8$  lattice with periodic boundary conditions. Let us label these zigzag chains using “bits,” 0 and 1, representing the  $x$  and  $y$  directions, respectively. The nine possible configurations are in Fig. 3(d). The zigzag chain of Fig. 2(b) is given by the periodic sequence “00101101,” and its energy is the lowest among the possible candidates, since it provides the largest band gap. When the electron-phonon interaction is adiabatically switched on, it is reasonable that the AFM phase Fig. 2(b) would still be stable for a finite  $\lambda$  range. Note that in Fig. 3(d), excited states characterized by other zigzag paths have small excitation energies, such as  $0.001 \sim 0.01$  in units of  $t_{aa}^x$ . Thus, at temperatures as low as a few degrees kelvin the ground state Fig. 2(b) can be easily distorted into other zigzag spin patterns. This fragility of the ground state may be related with the “spin glass” features observed in single-layer experiments [12], leading to an overall orbital disordered state. However, note that seven of the nine competing states, as well as the Z-AFM phase, have diagonal stripes. Then, even in a mixture of these states, the stripe direction is not random. Thus, it is possible that indications of diagonal charge stripes may be present in the “spin glass” phase of single-layer manganites.

In summary, novel striped charge-orbital ordering has been found in realistic models for manganites. Diagonal stripes in the FM phase have been observed at densities  $x = 1/m$ , with  $m$  an integer, and also in the CE-like Z-AFM phase. The orbital degree of freedom orders in a  $x = 0$  staggered pattern in between the stripes, playing a key role in stabilizing these structures, similarly as the real spin does for stripes in nickelates and cuprates. Our results have implications for the recently discovered short-range charge ordering effects in neutron scattering experiments, as well as for future experiments, particularly involving layered manganites.

The authors are grateful to P. Dai, M. Greven, J. Hill, and M. Kubota for useful comments. This work has been supported by the Ministry of Education, Science, Sports, and Culture of Japan, Fundación Antorchas, and Grant No. NSF-DMR-9814350.

- [1] See, e.g., *Colossal Magnetoresistive Oxides*, edited by Y. Tokura (Gordon & Breach, New York, 2000); E. Dagotto *et al.*, Phys. Rep. **344**, 1 (2001).
- [2] S. Yunoki *et al.*, Phys. Rev. Lett. **81**, 5612 (1998); A. Moreo *et al.*, Phys. Rev. Lett. **84**, 5568 (2000).
- [3] J.M. De Teresa *et al.*, Nature (London) **386**, 256 (1997); S.J.L. Billinge *et al.*, Phys. Rev. B **62**, 1203 (2000).
- [4] S. Shimomura *et al.*, Phys. Rev. Lett. **83**, 4389 (1999); P. Dai *et al.*, Phys. Rev. Lett. **85**, 2553 (2000); C.P. Adams *et al.*, Phys. Rev. Lett. **85**, 3954 (2000).
- [5] The propagation vector is in the pseudocubic notation.
- [6] L. Vasiliiu-Doloc *et al.*, Phys. Rev. Lett. **83**, 4393 (1999); M. Kubota *et al.*, J. Phys. Soc. Jpn. **69**, 1986 (2000).
- [7] T. Hotta *et al.*, Phys. Rev. B **60**, R15 009 (1999).
- [8] S. Yunoki *et al.*, Phys. Rev. Lett. **84**, 3714 (2000); T. Hotta *et al.*, Phys. Rev. B **62**, 9432 (2000).
- [9] T. Hotta *et al.*, Phys. Rev. Lett. **84**, 2477 (2000).
- [10] S. Kawano *et al.*, J. Phys. (Paris) Colloq. **49**, C8-829 (1988).
- [11] B.J. Sternlieb *et al.*, Phys. Rev. Lett. **76**, 2169 (1996); Y. Murakami *et al.*, Phys. Rev. Lett. **80**, 1932 (1998).
- [12] Y. Moritomo *et al.*, Phys. Rev. B **51**, R3297 (1995).
- [13]  $J_{AF}$  is small to make it compatible with experiments for the fully hole-doped  $\text{CaMnO}_3$  compound. See also L.F. Feiner and A.M. Oleś, Phys. Rev. B **59**, 3295 (1999).
- [14] Coulomb interactions are effectively included in the large  $\lambda$  regime (see T. Hotta *et al.* in Ref. [8]).
- [15] Here only the bond stretching mode is assumed to occur and  $\beta$  is set as 2, a realistic value deduced from vibration energies for breathing- and JT-mode phonons [7]. Note that in an isolated 2D sheet there is no constraint for  $u_i^z$ , the displacement of apical oxygens (AO), but the real 2D system is embedded in a 3D environment, suggesting that AO motion should be determined considering the influence of other ions between sheets. In this work, for simplicity,  $u_i^z$  is set to zero, assuming that AO are fixed in their positions by 3D effects.
- [16] J.M. Tranquada *et al.*, Nature (London) **375**, 561 (1995).
- [17] In the one-orbital model vertical/horizontal stripes have been obtained [see E. Dagotto *et al.* (Ref. [1]), Fig. III.d.6(b); H. Aliaga *et al.*, cond-mat/0011342].
- [18] S. Larochelle *et al.* (to be published); M. Greven (private communication).
- [19] Once the stripes melt, together with the dynamical aspect of the charge, the orbital order will no longer be long ranged but short. Then, melted stripes may lead to orbital liquid properties [M. Belesi *et al.* (to be published)].
- [20] For noncooperative calculations,  $\beta$  is set to  $\infty$ , while  $J_H = 20$  (but results at  $J_H = \infty$  are essentially the same).
- [21] At  $x = 1/3$  and large  $\lambda$ , the zigzag FM chain [Fig. 2(c)] is divided into small FM clusters for noncooperative JT phonons, while for cooperative case the Z-AFM phase [Fig. 2(c)] is stable. For large  $\lambda$ , the cooperative effect is crucial to stabilize the Z-AFM structure, as well as to observe the diagonal charge stripes in the FM phase.
- [22] Note that the charge density is nearly uniform at intermediate  $\lambda$  such as 1.2 in Fig. 3(c). In this interesting regime, a peak in the orbital correlations exists, while the analog in the charge sector is not prominent. Such an OO but CD  $x = 1/4$  state may be related to those observed in recent experiments for  $\text{Pr}_{1-x}\text{Ca}_x\text{MnO}_3$  (M. v. Zimmermann *et al.*, cond-mat/0007231).